

H α Objective Prism Survey of Abell 1060

S. M. Bennett¹ and C. Moss²

¹ Institute of Astronomy, Madingley Road, Cambridge, CB3 0HA, UK

² Blackett Laboratory, Imperial College of Science, Technology, and Medicine, Prince Consort Road, London, SW7 2BZ, UK

Received ;date; / Accepted ;date;

Abstract. As part of a continuing study of the effect of cluster environment on the star formation properties of galaxies, we have undertaken an H α objective prism survey of the nearby cluster, Abell 1060. We detect 33 galaxies in emission, 24 of which are cluster members. We present new radial velocity measurements and H α + [N II] equivalent widths and fluxes for a number of these galaxies. We distinguish between galaxies with diffuse and compact emission, the latter having been associated in previous work with a disturbed morphology of the galaxy and most likely resulting from tidally-induced star formation from galaxy–galaxy or cluster–galaxy interactions. The fraction of cluster spirals in Abell 1060 detected with compact emission agrees with the expected fraction for a cluster of its richness, as derived from results of a previous survey of 8 clusters. Some of the detected cluster early-type spirals exhibit anomalously high global H α equivalent widths, as compared to galaxies of similar type in the field.

Key words: Galaxies: clusters: general – Galaxies: clusters: individual: Abell 1060 – Galaxies: spiral – Galaxies: starburst

1. Introduction

The effect of cluster environment on the star formation properties of galaxies has long been a matter of debate. While some studies have suggested a lower star formation rate for cluster spirals as compared to the field (e.g. Gisler 1978; Dressler, Thompson, & Shectman 1985), other work has suggested a similar or enhanced rate, particularly for early-type spirals (e.g. Kennicutt, Bothum, & Schommer 1984; Gavazzi, Boselli, & Kennicutt 1991; Moss & Whittle 1993; Biviano et al. 1997). With the discovery that in distant rich clusters there is a high fraction of blue, star-forming galaxies, often with unusual morphology suggestive of mergers and tidal interactions (e.g. Lavery & Henry 1986; Thompson 1988; Couch et al. 1994), there is renewed interest in tidally-induced star formation by mergers and interactions in nearby clusters. In order to address these

issues, Moss, Whittle and co-authors have completed an objective-prism survey of eight nearby clusters of galaxies to detect global H α + [N II] emission as an indicator of the current rate of massive star formation. The survey technique is described by Moss, Whittle, & Irwin (1988), hereafter MWI, and initial results have been discussed by Moss & Whittle (1993) (see also Moss 1990; Moss et al. 1995; Moss & Whittle 1997; Moss, Whittle, & Pesce 1998). We have extended this survey to a ninth cluster, the Hydra I cluster, Abell 1060.

Abell 1060 is one of the nearest of the Abell clusters, at a redshift of $z \sim 0.01$, and is the nearest large cluster beyond the Virgo and Fornax clusters. It has a high spiral fraction (e.g. Solanes & Salvador-Solé 1992) and is a relatively poor cluster, with a low density intracluster medium (Loewenstein & Mushotzky 1996) and low X-ray luminosity (Edge & Stewart 1991). Since it is the nearest of the clusters surveyed by us so far, it can be surveyed to a fainter limit in absolute magnitude. However, its proximity means that it has a large projected diameter on the sky, with one Abell radius, $1 r_A = 2.3 = 1.5 h^{-1}$ Mpc (where h is defined in terms of the Hubble constant $H_0 = 100h$ km s⁻¹Mpc⁻¹). Whereas other clusters were surveyed in a region of radius $1.5 r_A$, the photographic plate size restricted survey of Abell 1060 to a region of radius somewhat less than one Abell radius (see §2.1). Richter (1989), hereafter R89, presents a catalogue of 581 galaxies in the cluster area, which contains a sample which is complete to the magnitude limit $V_{25} = 16.65$, within 2° of the cluster centre. This is a convenient complete sample for the present H α survey, extending to a fainter apparent magnitude than the Zwicky Catalogue used to define samples for other clusters.

Cluster properties are summarised in Table 1. The (B1950.0) position of the central cluster galaxy NGC 3311 is given as the cluster centre in columns 2 and 3. The mean heliocentric radial velocity $\langle v_\odot \rangle$ and velocity dispersion σ determined using N_{gal} individual galaxy redshifts are given in columns 4, 5, and 6 (Bird 1994). The Abell richness class (Abell, Corwin, & Olowin 1989) is given in column 7, the Bautz-Morgan and Rood-Shastry type

Table 1. Cluster properties

Name	R.A. (1950.0) 1	Dec. b	$\langle v_{\odot} \rangle$ km s $^{-1}$	σ km s $^{-1}$	N_{gal}	Richness	Type Class	
							B-M	R-S
(1)	(2)	(3)	(4)	(5)	(6)	(7)	(8)	(9)
Abell 1060 (Hydra I)	10 ^h 34 ^m 21 ^s .6 269°6	-27° 16' 05'' 26°49	3697	630	132	1	III	C

classes are given in columns 8 and 9 respectively (Bautz & Morgan 1970; Struble & Rood 1982).

The observations and data reduction are described in §2. Details of the observational technique are given in §2.1, and of the process of identifying the emission-line galaxies in §2.2, where a table of the detected emission-line galaxies (ELGs) is given. Measurements of radial velocities for the detected emission-line galaxies are presented in §2.3, and those of H α +N[II] equivalent widths and fluxes in §2.4, where measured H α +N[II] fluxes are also converted into effective star formation rates. A comparison of detected cluster emission-line galaxies in Abell 1060 with field galaxies and detected emission-line galaxies in other clusters is given in §2.5. Notes on individual galaxies are given in §2.6. Finally, we present a brief discussion of our results in §3.

2. Observations

2.1. Plate material

Observations were made with the 61/94 cm Curtis Schmidt at Cerro Tololo Inter-American Observatory equipped with a 6°+4° objective prism combination. The plate scale of the Curtis Schmidt is 96.6 arcsec mm $^{-1}$, with a usable field of 5° square. The dispersion at H α is 465 \pm 4 Å mm $^{-1}$, as determined in §2.3. At this moderate dispersion, the H α line is blended with the forbidden [N II] ($\lambda\lambda=6548, 6583$ Å) lines. Two exposures were made on hypersensitized IIIaF emulsion using an RG 630 filter. This combination of filter and emulsion gives an effective bandpass which has a FWHM of \sim 350 Å centred on 6655 Å with a peak sensitivity at \sim 6717 Å (MWI). At the relatively low redshift of the Hydra cluster, [S II] ($\lambda\lambda=6716, 6731$ Å) emission can also be detected.

Repeated exposures of the same field taken with opposite dispersion directions are useful to confirm the reality of emission features allowing both elimination of spurious detections, and confirmation of weak emission features, particularly in cases where the underlying continuum is too faint to be seen. Reversing the dispersion direction also enables redshift determination (see MWI). The see-

ing is critical to the detection of emission. Details of the exposures, both taken under good seeing conditions, are given in Table 2.

The fields covered by the two plates are not exactly coincident. The plate boundaries are shown in Fig. 1 as solid boxes. The coverage of R89 is also shown: the dashed box shows the area covered by the catalogue, the dashed circle the area within which it is complete to the magnitude limit $V_{25} = 16.65$. One Abell radius is indicated by the dotted circle. There are three distinct regions in Fig. 1: the region in which the plates overlap, the region covered by only one plate, and the region within which R89 is complete. The complete region is contained entirely within the overlap region.

2.2. Identification of emission-line galaxies

The plates were searched systematically for galaxies showing H α emission using a low-power binocular microscope. A visibility parameter (S strong, MS medium-strong, M medium, MW medium-weak, or W weak) describing how readily the emission is seen on the plate, and a concentration parameter (VD very diffuse, D diffuse, N normal, C concentrated, or VC very concentrated) describing the spatial distribution of the emission and the contrast with the underlying continuum, were assigned to each candidate following the scheme of MWI. Within the overlap region galaxies were only accepted as emission-line sources if they had been independently detected on both plates and the separate emission features were consistent with each other. Outside the overlap area, galaxies were accepted only if they showed strong emission. Galaxies detected in H α are listed in Table 3 in order of increasing Right Ascension.

In order to construct a complete sample of surveyed galaxies for statistical analysis, it is necessary to correct for the effect of overlapping spectra. This is a particular problem at the relatively low galactic latitude ($b = 26^\circ 5'$) of Abell 1060. All galaxies within the region of completeness of R89 brighter than the limiting magnitude $V_{25} = 16.65$ were checked on both plates to ensure that

Table 2. Objective prism plates

Plate number	U.T. date	Plate centre R.A. (1950.0) Dec.		Filter	Emulsion	Exp. min.	Prism	Apex N/S
(1)	(2)	(3)	(4)	(5)	(6)	(7)	(8)	(9)
29132	Feb 23 1985	10 ^h 34 ^m	-27 ^o .5	RG 630	IIIaF	100	6 ^o +4 ^o	N
29133	Feb 23 1985	10 34.5	-27.3	RG 630	IIIaF	100	6+4	S

their spectra were not overlapped by those of nearby objects. Table 4 lists both the identifications in R89 of the galaxies included in the complete sample, and those of galaxies which are deemed not to have been surveyed due to overlapping spectra. Those in the former list can be regarded as being confirmed as non emission-line galaxies if they do not appear in the table of detected emission-line galaxies (Table 3).

The objective prism spectra of the detected emission-line galaxies were digitised using the PDS (Plate Density Sensitometer) facility at the Royal Greenwich Observatory in order to measure line redshifts, equivalent widths, and fluxes.

2.3. Redshift determinations

As demonstrated by MWI, after Stock & Osborn (1980), it is possible to obtain redshift estimates for emission-line galaxies accurate to within a few hundred km s⁻¹ using two Schmidt telescope objective prism plates taken with opposite dispersion directions. Following the method detailed in MWI, we obtained redshift estimates for all detected emission-line galaxies which we calibrated against available redshifts from the literature. Assuming that the dispersion of the prism combination is approximately constant over the narrow wavelength range of interest, the slope of this calibration gives a value for the dispersion of the 6^o+4^o prism combination of 465±4 Å mm⁻¹ between 6600 and 6800 Å. The rms scatter about this relation of ~340 km s⁻¹ is slightly larger than that found by MWI of ~205 km s⁻¹; this may be partly due to the fact that MWI used a two-dimensional cross-correlation technique, whereas we used the one-dimensional analogue.

Heliocentric velocities determined using the two-plate technique for seven galaxies which do not have existing redshift determinations and the emission associated with the superposed galaxies NGC 3314 (see §2.6) are listed in Table 5.

Table 5. Redshifts of emission-line galaxies

No.	Galaxy name	v_{\odot} km s ⁻¹
(1)	(2)	(3)
2	R89 101	4800
13	NGC 3314A	2600
19	WPV 78	3000
27	R89 483	11500
28	ESO 437-G43	4100
29	R89 525	11200
30	AM 1043-285	9600
33	ESO 437-G64	4000

2.4. Equivalent widths and fluxes

The two-dimensional digitised spectral scans were reduced to one-dimensional spectra. These were used to determine equivalent widths of the blended H α + [N II] emission lines using the dispersion value derived from the two-plate redshift determinations (§2.3 above).

It was only possible to measure a reliable equivalent width for 13 of the 33 emission-line galaxies. Other galaxies had spectra which were overlapped by those of other objects, or emission or continuum which was too faint, or too diffuse, to be measured reliably.

Comparison between equivalent widths measured from the two plates shows a mean difference of 0(±3) Å for the 11 galaxies for which equivalent widths were measured on both plates. The mean measured equivalent widths (W_{λ}) are listed in column 3 of Table 6. A colon appended to the equivalent width value indicates some additional uncertainty in fitting the continuum.

H α + [N II] fluxes were measured in arbitrary units of photographic density, which is approximately proportional to intensity. We then used the flux calibration of Bessell (1979) to give H α + [N II] fluxes from the R magnitudes,

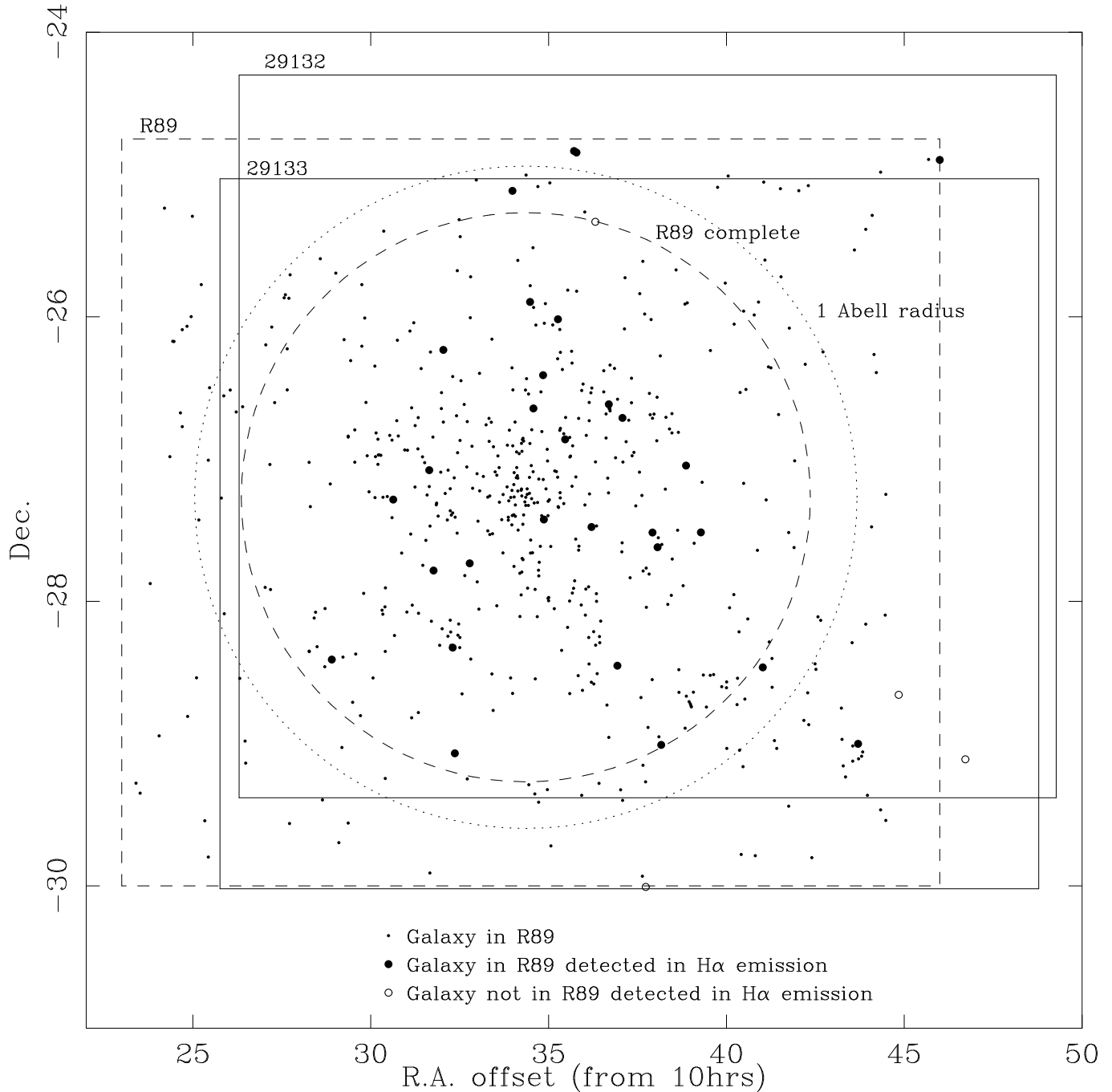


Fig. 1. Survey coverage. Plate boundaries are indicated by solid lines. The area covered by R89 is shown by the dashed box, the area within which it is complete by the dashed circle. The dotted circle has a radius of $1.5 h^{-1} \text{ Mpc}$ (1 Abell radius) and is centred on the central cluster galaxy NGC 3311. Galaxies in R89 are shown as dots, detected emission-line galaxies as filled and open circles.

where available in the literature, and the equivalent width measurements. These flux values were used to calibrate the photographic fluxes, which were then converted to luminosities using corrections for galactic extinction from Burstein & Heiles (1984) and the NASA Extragalactic Database (NED), the internal extinction correction given by de Vaucouleurs et al. (1991), and a distance corre-

sponding to the cluster mean redshift for cluster members, or individual galaxy redshifts for background galaxies, using the velocity correction for Virgocentric infall given in R89 (Richter, Tammann, & Huchtmeier 1987). H_0 was taken as $50 \text{ km s}^{-1} \text{ Mpc}^{-1}$. The scatter in this calibration is ~ 0.08 in the log, corresponding to an uncertainty of $\sim 20\%$ in luminosity.

Table 3. Galaxies with detected H α emission

No.	Catalogue name			R.A. (1950.0)	Dec.	V	Type	H α emission		v_{\odot} km s $^{-1}$	Notes
	R89 W85	ESO NGC	IRAS Arp					Vis.	Conc.		
(1)	(2)	(3)	(4)	(5)	(6)	(7)	(8)	(9)	(10)	(11)	(12)
1	57		10288-2824	10 ^h 28 ^m 54 ^s .2	-28° 24' 31''	15.33	... SABa	MW	N	3689	
2	101			10 30 38	-27 17.1	15.86	E	W	N	4800 ^a	
3	128	501-G16	10316-2704	10 31 38.7	-27 04 40	14.14	SBab(rs) SBa	MW	C	9683	
4	135			10 31 46	-27 47 01	15.39	SB pec	W	N	3398	
5	144	501-G17	10320-2613	10 32 2.4	-26 13 56	14.18	S0(7) Sa(sp)	MS	C	4429	
6	158	436-IG42	10323-2819	10 32 18.3	-28 19 28	14.80	E4: IG	S	VC	3447	*
7	161	436-G43		10 32 21.9	-29 04 03	15.45	S...	MW	N	9123	*
8	181	437-IG3		10 32 46.9	-27 43 58	15.13	S pec	MW	D	2391	*
9	229	501-G32		10 33 59	-25 06.9	14.26	SBb(r) pec	MS	C	3933	*
10	281			10 34 28.8	-25 53 42	15.17	Sa	M	N	3686	
11	291			10 34 34.5	-26 38 36	15.96	S pec	M	C	3170	
12	310	501-G45	10348-2624	10 34 50.8	-26 24 38	14.41	S0(3)/a(r) SAB(s)a	M	N	4578	*
13	312	501-IG46	10348-2725	10 34 51.9	-27 25 27	13.11	S(B)c (IG)	S	C	2851	*
14	335	501-G53	10352-2600	10 35 15.9	-26 01 00	14.26	Sa: Sa	MS	D	3814	
15	348	501-G59	10354-2651	10 35 28	-26 51 40	13.55	Sa SAa	MS	N	2385	
16*	363	501-IG61		10 35 43	-24 50.1	...	"Multiple"	S	N	3597	*
17*	367	501-G62		10 35 47	-24 50.7	...	Sb	S	N	10200 ^a	*

The H α + [N II] luminosities from this calibration were corrected to give H α luminosities using the conversion of $W_{\lambda}(\text{H}\alpha + [\text{N II}]) = 1.33W_{\lambda}(\text{H}\alpha)$ from Kennicutt (1983). This was then converted to an effective star formation rate using the conversion factor of Alonso-Herrero et al. (1996) of $L(\text{H}\alpha)/\text{SFR} = 3.10 \times 10^{41} \text{erg s}^{-1}/M_{\odot} \text{yr}^{-1}$, which corresponds to a Salpeter (1955) IMF with upper and lower mass cutoffs of $125 M_{\odot}$ and $0.1 M_{\odot}$ respectively. This conversion is highly IMF dependent.

Calibrated H α + [N II] fluxes and effective star formation rates are listed in columns 4 and 5 of Table 6. A star

formation rate is not listed for NGC 3393 as it is a Seyfert. Despite the uncertainties in the star formation rate determination, the derived values of between a tenth of a solar mass and a few solar masses per year lie within the range expected for normal spirals. Nevertheless, a few galaxies appear to have an anomalously high star formation rate for their morphological type (see §2.5).

Table 3. Continued

No.	Catalogue name			R.A. (1950.0)	Dec.	V	Type	H α emission		v_{\odot} km s $^{-1}$	Notes
	R89 W85	ESO NGC	IRAS Arp					Vis.	Conc.		
(1)	(2)	(3)	(4)	(5)	(6)	(7)	(8)	(9)	(10)	(11)	(12)
18	390 77	501-G65	10361-2728 1036-272	10 ^h 36 ^m 12 ^s .3	-27° 28' 37''	13.37	Sbc Irr	MS	D	4378	*
19	78			10 36 18.9	-25 19 55	MW	C	3000 ^a	
20	413 79	501-G67	10366-2636	10 36 41.7	-26 36 54	15.05	SBa(s) SBa	MW	N	10594 ^b	
21	420		10369-2827	10 36 56.1	-28 27 08	15.83	S0(3) S0/a	W	N	2811	
22	425	501-G70	10370-2642	10 37 4.5	-26 42 40	14.99	SBa(rs) SB(r)0/a	M	C	10707	
23*		437-G35	10377-3000	10 37 44	-30 00 24	...	SB(s)bc: SABa	S	VC	3396 ^c	*
24	457	437-G36 3336	10379-2730 1037-273	10 37 55.4	-27 30 58	12.19	S(B)c(rs) SAc	MW	D	3940	*
25	461		F10381-2737 1038-273	10 38 3.9	-27 37 12	14.26	S0(2)	MW	N	4503	*
26	465	437-IG37		10 38 10	-29 00.5	15.98	“Double”	M	N	3600 ^a	
27	483		F10388-2702	10 38 52	-27 02.7	16.05	S	M	N	11500 ^a	
28	492	437-G43		10 39 17	-27 30.9	16.43	SB...	M	N	4100 ^a	
29	525 82			10 41 1.4	-28 27 49	16.53	S	W	N	11200 ^a	
30	564			10 43 42	-29 00.1	15.23	S	MW	D	9600 ^a	
31			1043-285 10448-2839	10 44 50.7	-28 39 23	15.5	... SBb	S	VC	10235 ^d	
32*	581 84	501-G100 3393	10459-2453 1045-245	10 46 0	-24 53.8	...	Sa SAab	S	C	3720	*
33		437-G64	F10466-2906	10 46 43	-29 06 36	...	Sb ²	W	N	4000 ^a	

2.5. Cluster emission-line galaxies

From the distribution of detected emission-line galaxies with magnitude it appears that the complete survey sample ($V \leq 16.65$, $r < 2^\circ$) extends somewhat below the detection limit of the H α survey, although this detection limit is not well defined. For the magnitude ranges, $12 < V \leq 14$, $14 < V \leq 16$, and $V > 16$ the percentages of galaxies, types Sa and later, detected in emission are 24%, 23% and 6% respectively. We estimate that emission-line galaxy detections are reasonably complete to $V=16$. Accordingly in what follows, we restrict discussion to a subsample of the complete sample, with $V \leq 16$, $r < 2^\circ$. There are some 180 galaxies in this subsample which have been surveyed

for H α emission, of which 35 are classified in R89 as E or E/S0, 62 as S0 or S0/a, and 65 as Sa or later, with 8 being unclassified. The percentages of the three type groups detected in emission are 6%, 4% and 23% respectively. As expected, only a small percentage of early type galaxies were detected in emission.

Previous work (Moss & Whittle 1993) has shown the usefulness of a distinction between *diffuse* emission described by the concentration classes D (diffuse) and VD (very diffuse), and *compact* emission described by the other three classes VC (very concentrated), C (concentrated), and N (normal). It has been found that compact emission is strongly associated with a disturbed morphology of the galaxy, and most likely results from tidally-

Table 3. Notes to the Table

Column 1. Identification number. An asterisk indicates that the object lies outside the overlap region and has therefore only been detected on one plate.

Column 2. Line 1, identification in R89. Line 2, identification in Wamsteker et al. (1985).

Column 3. Line 1, identification in Lauberts (1982). Line 2, NGC number.

Column 4. Line 1, IRAS identification from Wang et al. (1991) or NED. Line 2, identification in Arp & Madore (1987).

Columns 5 & 6. (B 1950.0) Right Ascension and Declination. These are taken from R89 except no. 19 (Wamsteker et al. 1985), no. 23 (Lauberts 1982), no. 31 (van Driel, van den Broek, & de Jong 1991), no. 33 (Lauberts 1982) and are quoted to the same precision as the source.

Column 7. V magnitude, V_{25} from R89.

Column 8. Morphological types from R89 (line 1) and Wang et al. (1991) (line 2) except no. 33 (Lauberts 1982). Wang’s types should be more reliable than Richter’s as they are based on a UK Schmidt IIIaJ plate. Note, though, that Wang’s identification of the galaxy pair NGC 3314 as IG (interacting galaxy) is misleading (see text).

Column 9. Visibility parameter (S strong, MS medium-strong, M medium, MW medium-weak, W weak).

Column 10. Concentration parameter (VD very diffuse, D diffuse, N normal, C concentrated, VC very concentrated).

Column 11. Heliocentric velocity. From R89, otherwise superscript indicates a) this paper, b) de Vaucouleurs et al. (1991), c) Mathewson, Ford, & Buchhorn (1992), d) Strauss et al. (1992).

Column 12. An asterisk indicates a note: *No. 7* appears to be tidally distorted. Lauberts (1982) notes “bright centre, faint disturbed envelope.” *No. 8* has an apparently double nucleus, and could be a merger remnant. *No. 9* has peculiar morphology, exhibits several distinct emission regions. *No. 12* is asymmetric. Lauberts (1982) notes an “extremely faint ring.” *No. 18*, noted by Arp & Madore (1987) as a disturbed spiral, has a peculiar morphology and may have been tidally disrupted. Several emission regions are visible. *No. 23* is noted as disturbed by Lauberts (1982) and ascribed “thick arms, knots, and dust patches, optical pair” by Corwin, de Vaucouleurs, & de Vaucouleurs (1985). *No. 24*, NGC 3336, is a face-on Sc galaxy, with many individual HII regions visible in emission. *No. 25* is noted by Arp & Madore as “close pair, end of chain.” *No. 32*, NGC 3393, is a type 2 Seyfert (Storchi-Bergmann, Kinney, & Challis 1995). *Nos. 6, 13, 16, & 17* see §2.6.

Table 6. Global H α + [N II] equivalent widths and fluxes

No.	Galaxy name	W_λ Å	$f \times 10^{14}$ ergs cm $^{-2}$ s $^{-1}$	SFR M $_\odot$ yr $^{-1}$
(1)	(2)	(3)	(4)	(5)
1	R89 57	19:	6	0.1
5	ESO 501-G17	23:	16	0.4
6	ESO 436-IG42	96	85	1.4
7	ESO 436-G43	52	16	1.8
8	ESO 437-IG3	59	17	0.4
9	ESO 501-G32	42	40	0.6
10	R89 281	49	19	0.3
12	ESO 501-G45	21:	10	0.2
16	ESO 501-IG61	31	11	0.2
18	ESO 501-G65	53	92	1.7
22	ESO 501-G70	19:	8	1.3
31	IRAS 10448-2839	38:	37	4.8
32	NGC 3393	39	148	...

induced star formation from galaxy–galaxy or cluster–galaxy interactions. Furthermore there is a strong correlation between cluster mean central galaxy density and the fraction of galaxies of types Sa and later with compact emission (Moss & Whittle 1997). This is illustrated in Fig. 2, where the central galaxy density is calculated

from the number of galaxies with absolute magnitude $M_{T,0} \leq -20.4$ within $0.5r_A$ of the cluster centre, corrected for the effects of foreground and background contamination and cluster galaxies projected onto the central region. For Abell 1060, the central galaxy density calculated in this way is approximately 1.2 Mpc^{-3} . However, the actual value is likely to be lower than this as the correction for projection was less accurate than was possible for more distant clusters. Within 120 arcmin ($\sim 1 r_A$) of the cluster centre 8 galaxies (14%) of types Sa and later have compact emission. This is in good agreement with the fraction of 12% for the lowest density bin in Fig. 2, indicating that the number of spirals detected with compact emission in Abell 1060 agrees with the expected value for a cluster of its richness.

A detailed comparison between the star formation rates of cluster galaxies in Abell 1060 and corresponding rates for field galaxies is not possible due both to the small sample of detected emission-line galaxies and incomplete measurements of H α equivalent widths. Nevertheless it may be noted that a significant fraction of the detected cluster emission-line galaxies are early-type spirals which may be surprising in view of the detection limit of the survey technique of $\sim 20 \text{ \AA}$ (see MWI), and the expectation that H α equivalent widths for galaxies of types Sab and earlier in the field are less than 20 \AA (Kennicutt & Kent 1983). Indeed, the three galaxies ESO 501-G17, ESO 501-G45, and R89 281, typed Sa or earlier by R89 and Wang et al. (1991), and known cluster members, have measured equivalent widths greater than 20 \AA ,

Table 4. Identifications in R89 of galaxies included in the complete sample

Galaxies surveyed																		
32	33	34	35	36	37	45	46	47	48	49	50	51	54	55	56	57	58	61
62	64	65	66	67	69	70	71	72	73	74	75	76	77	78	79	80	81	82
83	85	86	88	90	91	94	97	98	99	100	101	103	104	105	106	109	110	112
113	114	115	116	117	119	120	121	122	124	126	128	129	131	132	133	134	135	138
139	144	145	148	149	150	154	155	156	158	161	162	164	165	166	167	168	169	171
174	175	177	179	181	182	185	186	188	189	190	191	192	193	194	196	198	202	203
204	206	208	209	210	211	212	213	214	215	216	217	218	219	220	221	222	224	225
226	227	232	233	234	236	237	238	239	241	243	244	245	246	247	249	252	253	254
255	256	258	260	261	264	266	268	269	271	273	274	278	279	281	282	283	286	288
289	290	291	292	293	295	296	297	299	303	305	306	307	308	310	312	313	314	316
317	319	320	322	325	327	329	333	334	335	336	338	339	340	341	342	343	344	345
347	348	351	353	357	358	359	360	365	368	369	373	375	376	377	379	381	384	385
386	387	389	390	391	396	397	400	403	405	407	409	413	416	418	419	420	421	423
425	427	428	431	433	437	439	440	443	445	446	450	453	457	461	463	464	465	466
469	471	474	475	477	478	479	480	481	482	483	484	485	486	487	489	490	491	492
493	494	495	496	497	498	500	502	506	507	509	511	513	516	517	519	520	521	523
525	528	529	530	531	532	540	546											

Galaxies not surveyed due to overlapping stellar spectra																		
40	41	84	123	141	159	170	173	183	205	223	228	230	231	250	287	311	330	337
371	372	383	394	412	429	455	468	501	503	508	510	536	542					

and can therefore be considered to have unusually high star formation rates. The cluster elliptical ESO 436-IG42 also has a very high equivalent width of 96 Å (see §2.6). These results are consistent with an enhanced star formation rate in early-type cluster spirals found previously for other clusters (see Moss & Whittle 1993).

2.6. Notes on individual galaxies

No. 6, ESO 436-IG42: This galaxy is clearly interacting with a nearby companion; they are joined by a bridge of material (Lauberts 1982). The fact that it is classified as an elliptical and exhibits compact emission points to the possibility of a centrally-concentrated burst of star formation triggered by this interaction.

No. 13, NGC 3314A: This is the foreground member of the remarkable superposed galaxy pair NGC 3314, discussed in detail by Schweizer & Thonnard (1985) and Richter, Materne, & Huchtmeier (1982), which consists of two spiral galaxies of comparable angular size, one face-on and the other more nearly edge-on, whose centres are superposed almost exactly along the line of sight. Two redshifts have been determined for the pair from optical and 21 cm line measurements of 2 851 and 4 641 km s⁻¹. Both sets of authors identify NGC 3314A as both the fore-

ground object (dust lanes in its disk obscure NGC 3314B) and as having the lower recession velocity. The two-plate redshift estimate (see §2.3) of $2\,600 \pm 340$ km s⁻¹ confirms that emission is detected in the foreground NGC 3314A, in agreement with the spectrum of Schweizer & Thonnard (1985).

Nos. 16 & 17, ESO 501-IG61 & 501-G62: These two galaxies are seen in close separation on the sky, ~ 1 arcmin apart, and might consequently be taken for an interacting pair. As they lie outside the overlap area, a two-plate redshift measurement was not possible. However, a less accurate estimate can be made using a single plate, giving redshifts of $\sim 3\,200$ km s⁻¹ for ESO 501-IG61 and $\sim 10\,200$ km s⁻¹ for ESO 501-G62, with an adopted uncertainty of ~ 550 km s⁻¹ (MWI). This is accurate enough to identify ESO 501-IG61 as a possible cluster member and ESO 501-G62 as a non-member, and to confirm that they are not an interacting pair as might otherwise be inferred from their close separation. The R89 value of 3 597 km s⁻¹ has been adopted for the redshift of ESO 501-IG61.

3. Discussion and conclusions

We have surveyed the Hydra cluster, Abell 1060, for star-forming galaxies using an objective prism technique to de-

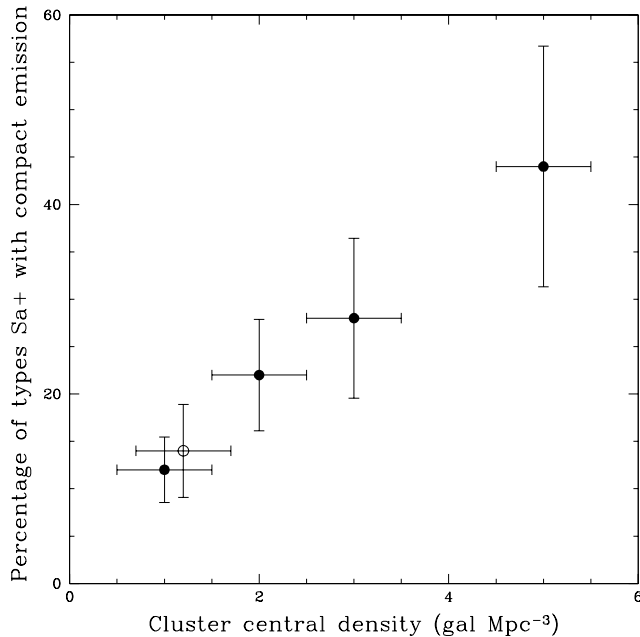


Fig. 2. The percentage of galaxies of types Sa and later showing compact emission plotted as a function of cluster central galaxy density. Filled circles indicate the eight clusters studied by Moss & Whittle (1997), the open circle indicates Abell 1060. Error bars indicate Poisson errors.

tect H α emission. We detect a total of 33 ELGs in the survey area, all of which have been identified with previously-known objects from one or more of a variety of catalogues. Radial velocities have been determined for 7 ELGs without previous determinations, and measurements have been made of global H α +N[II] equivalent width and flux values for 13 ELGs. For a complete galaxy sample ($n=180$) with $V \leq 16$ within 2° of the cluster centre, 24 galaxies are detected in emission, of which 18 are cluster members.

In accord with previous work (MWI) we have classified the appearance of the emission as compact or diffuse. It has previously been found that compact emission is associated with a disturbed galaxy morphology, and is most likely the result of tidally-induced star formation either by galaxy–galaxy or cluster–galaxy interactions (see Moss & Whittle 1993). Furthermore the fraction of spirals in a cluster with compact emission has previously been found to correlate with cluster richness (see Moss & Whittle 1997). Using the complete galaxy sample we show that the fraction of spirals detected with compact emission in Abell 1060 is consistent with this correlation.

Finally, although the small sample of detected cluster ELGs in Abell 1060 precludes a detailed comparison of star formation rates between these cluster galaxies and corresponding types in the field, it is to be noted that at least three early-type cluster spirals (types S0 to Sa) and an elliptical have global H α equivalent widths greater than

20 Å, which would be anomalously high for these galaxy types in the field. This is consistent with an enhanced star formation rate in early-type cluster spirals found in previous work (Moss & Whittle 1993).

Acknowledgements. We thank V.M. Blanco who generously provided the plate material on which this study is based. SMB is supported by the Particle Physics and Astronomy Research Council. CM thanks the Institute of Astronomy, Cambridge for support during the course of this project. This research has made use of the NASA/IPAC Extragalactic Database (NED) which is operated by the Jet Propulsion Laboratory, Caltech, under contract with the National Aeronautics and Space Administration. Cerro Tololo Inter-American Observatory, National Optical Astronomy Observatories, are operated by the Association of Universities for Research in Astronomy, under contract with the National Science Foundation.

References

- Abell G. O., Corwin H. G., Olowin R. P., 1989, *ApJS*, 70, 1
 Alonso-Herrero A., Aragón-Salamanca A., Zamorano J., Rego M., 1996, *MNRAS*, 278, 417
 Arp H. C., Madore B. F., 1987, *A Catalogue of Southern Peculiar Galaxies and Associations*. Cambridge University Press, Cambridge
 Bautz L. P., Morgan W. W., 1970, *ApJ*, 162, L149
 Bessell M. S., 1979, *PASP*, 91, 89
 Bird C. M., 1994, *AJ*, 107, 1637
 Biviano A., Katgert P., Mazure A., et al., 1997, *A&A*, 321, 84
 Burstein D., Heiles C., 1984, *ApJS*, 54, 33
 Corwin Jr., H. G., de Vaucouleurs A., de Vaucouleurs G., 1985, *Southern Galaxy Catalogue*. University of Texas, Austin
 Couch W. J., Ellis R. S., Sharples R. M., Smail I., 1994, *ApJ*, 430, 121
 Dressler A., Thompson A. B., Shectman A., 1985, *ApJ*, 288, 481
 van Driel W., van den Broek A. C., de Jong T., 1991, *A&AS*, 90, 55
 Edge A. C., Stewart G. C., 1991, *MNRAS*, 252, 428
 Gavazzi G., Boselli A., Kennicutt R., 1991, *AJ*, 101, 1207
 Gisler G. R., 1978, *MNRAS*, 183, 633
 Kennicutt R. C., 1983, *ApJ*, 272, 54
 Kennicutt R. C., Bothun G. D., Schommer R. A., 1984, *AJ*, 89, 1279
 Kennicutt R. C., Kent S. M., 1983, *AJ*, 88, 1094
 Lauberts A., 1982, *The ESO/Uppsala Survey of the ESO(B) Atlas*. ESO, Garching
 Lavery R. J., Henry J. P., 1986, *ApJ*, 304, L5
 Loewenstein M., Mushotzky R. F., 1996, *ApJ*, 471, L83
 Mathewson D. S., Ford V. L., Buchhorn M., 1992, *ApJS*, 81, 413
 Moss C., 1990. In: Sulentic J. W., Keel W. C., Telesco C. M. (eds.) *Paired and Interacting Galaxies*. IAU Colloq. No. 124, Kluwer, Dordrecht, Holland, p. 327
 Moss C., Whittle M., 1993, *ApJ*, 407, L17
 Moss C., Whittle M., 1997. In: *Starburst Activity in Galaxies*. *Rev. Mex. Astron. Astrofis. Conf. Ser.* Vol. 6, p. 145
 Moss C., Whittle M., Irwin M. J., 1988, *MNRAS*, 232, 381
 Moss C., Whittle M., Pesce J. E., 1998, *MNRAS*, submitted

- Moss C., Whittle M., Pesce J. E., Socas-Navarro H., 1995, *Astrophys. Lett. Commun.*, 31, 215
- Richter O.-G., 1989, *A&AS*, 77, 237
- Richter O.-G., Materne J., Huchtmeier W. K., 1982, *A&A*, 111, 193
- Richter O.-G., Tammann G. A., Huchtmeier W. K., 1987, *A&A*, 171, 33
- Salpeter E. E., 1955, *ApJ*, 121, 161
- Schweizer F., Thonnard N., 1985, *PASP*, 97, 104
- Solanes J. M., Salvador-Solé E., 1992, *ApJ*, 395, 91
- Stock J., Osborn W., 1980, *AJ*, 85, 1366
- Storchi-Bergmann T., Kinney A. L., Challis P., 1995, *ApJS*, 98, 103
- Strauss M. A., Huchra J. P., Davis M., et al., 1992, *ApJS*, 83, 29
- Struble M. F., Rood H. J., 1982, *AJ*, 87, 7
- Thompson L. A., 1988, *ApJ*, 324, 112
- de Vaucouleurs G., de Vaucouleurs A., Corwin H. G., et al., 1991, *Third Reference Catalogue of Bright Galaxies*. Springer, New York
- Wamsteker W., Prieto A., Vitores A., et al., 1985, *A&AS*, 62, 255
- Wang G., Clowes R. G., Leggett S. K., MacGillivray H. T., Savage A., 1991, *MNRAS*, 248, 112